JOURNAL OF GUIDANCE, CONTROL, AND DYNAMICS
Vol. 20, No. 6, November–December 1997

Modeling Fluid–Structure Interaction

José L. Ortiz* and Alan A. Barhorst†
Texas Tech University, Lubbock, Texas 79409-1021

A methodology for modeling the dynamics of a structure interacting with a fluid having a free surface is addressed. In this context, a structure is either a single rigid container or a rigid container coupled to a flexible multibody system. All nonlinearities inherent in the dynamics of the structure are taken into account. Two models used to handle the fluid are described. The first model assumes an incompressible viscous fluid, and the second utilizes potential flow with modified Rayleigh damping. Nonlinear sloshing effects are considered, and no simplifications are made on the field equations and boundary conditions. The end result of the methodology is a set of first-order differential equations for the motion of both the structure and the fluid. Emphasis is placed on the point that the motion of the structure is not prescribed but is found as part of the solution procedure. Numerical examples and experimental results justifying the approach are presented.

I. Introduction

In the literature, fluid–structure interaction problems involving a free surface can be classified as follows: 1) rigid containers carrying a fluid with a free surface, 2) rigid floating bodies, and 3) submerged rigid bodies moving close to a free surface (see Fig. 1). However, the majority of solutions deal with a known prescribed motion for the container or moving body or linearizations on the free surface. If the fluid is modeled with the Navier–Stokes equations, numerous strategies have as their primary numerical tool either finite differences,[1–6] the finite element method (FEM),[7] or the boundary element method (BEM).[8,9] When the fluid was modeled with potential flow theory, a handful of investigators used the FEM,[10–12] whereas many preferred using the BEM with standard numerical integration procedures.[13–27]

In contrast, there is little published information on the true fluid–structure interaction problem, including nonlinear sloshing effects, where true interaction is defined as interaction in which both the motion of the structure and the motion of the fluid are found in the numerical procedure. For example, Lui and Lou[28] present a true interaction solution for a one-degree-of-freedom structure, but sloshing effects are linearized and the structure must have linear behavior; the solution is expedited via Laplace transforms. Simple solutions for the case of a rigid floating body are presented in the literature,[13,29,30] as are approximate approaches.[31–34]

The objective of this work is to model true fluid–structure interaction, including nonlinear sloshing effects. In the context of this paper, a structure means either a single rigid container or a rigid container coupled to a complex multibody system, where each body is either rigid or flexible. All nonlinearities inherent in the dynamics of the structure are taken into account, with no simplifications made on its behavior; material and geometric nonlinearities in the flexible bodies can be considered. Two models used to handle the fluid are described. The first model assumes an incompressible viscous fluid; the second utilizes potential flow with modified Rayleigh damping. All nonlinearities due to boundary conditions or sloshing effects are considered. Other incompressible fluid models could be implemented analogously.

The end result of the methodology introduced herein is a set of first-order differential equations for the motion of both the structure and the fluid. Numerical examples and experimental results justifying the approach are presented.

Received Sept. 10, 1996; presented as Paper 97-0785 at the AIAA 35th Aerospace Sciences Meeting, Reno, NV, Jan. 6–9, 1997; revision received Jan. 25, 1997; accepted for publication Jan. 31, 1997.

*Visiting Assistant Professor, Mechanical Engineering Department.
†Assistant Professor, Mechanical Engineering Department. Member AIAA.

II. Mathematical Model

Without loss of generality, the description of the methodology is provided in connection with the two-dimensional problem shown in Fig. 1a. The methodology consists of three steps. The first is to find the equations of motion for the structure as functions of the interaction pressure (see Fig. 2). The second consists of building a boundary-value problem for the pressure as a function of the acceleration of the structure. The third step deals with coupling the pressure solution with the equations of motion of the structure. No details are given on obtaining the equations of motion for the structure. These can be found by any suitable methodology, such as Newton's method, Lagrange's method, Hamilton's principle, Kane's approach,[35,36] or the method presented by Barhorst and Everett.[37] The first fluid model to be considered assumes incompressible viscous flow.

A. Incompressible Viscous Flow

1. Equation of Motion of the Structure

In general, for the structure shown in Fig. 2, the equations of motion are a set of coupled ordinary and partial differential equations. After discretization (FEM, BEM, etc.), these equations take the form

$$[M]_{n\times n}\{\dot{U}_s\}_{n\times 1} = \{R(U_s, Q_s, p)\}_{n\times 1} \tag{1}$$

$$\{\dot{Q}_s\}_{n\times 1} = [C]_{n\times n}\{U_s\}_{n\times 1} \tag{2}$$

The U_s are generalized speeds corresponding to n independent generalized coordinates Q_s describing the configuration of the structure; $[M]$ and $[C]$ are the mass and kinematic matrices, whereas $\{R(U_s, Q_s, p)\}$ is a load vector that depends on the pressure field p yet unknown.

2. Field Equation for the Pressure

The Navier–Stokes equation in the fluid domain V_f (Fig. 3) is

$$\rho\left(\frac{\partial \boldsymbol{V}}{\partial t} + \boldsymbol{V}\nabla\boldsymbol{V}\right) = -\nabla p + \rho\boldsymbol{f} + \rho\nu\nabla^2\boldsymbol{V} \quad \text{in} \quad V_f \tag{3}$$

Here, $\boldsymbol{V}$ is the absolute velocity of a fluid particle as observed in the Newtonian frame N. The density is ρ, $\boldsymbol{f}$ is the body force per unit mass, and ν is the kinematic viscosity. Assuming that ρ is constant and $\nabla\cdot\boldsymbol{f} = 0$, the combination of these expressions with the zero divergence condition yields[38]

$$\nabla^2 p = -\rho\nabla\cdot(\boldsymbol{V}\nabla\boldsymbol{V}) \quad \text{in} \quad V_f \tag{4}$$

3. Boundary Conditions for the Pressure

On the free surface S_f, the following dynamic boundary condition holds:

$$p = 0 \quad \text{on} \quad S_f \tag{5}$$

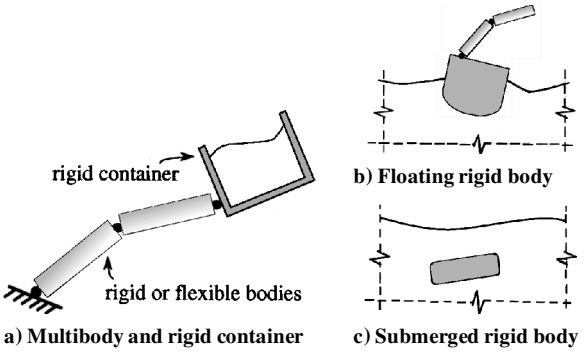

Fig. 1 Some fluid–structure interaction problems.

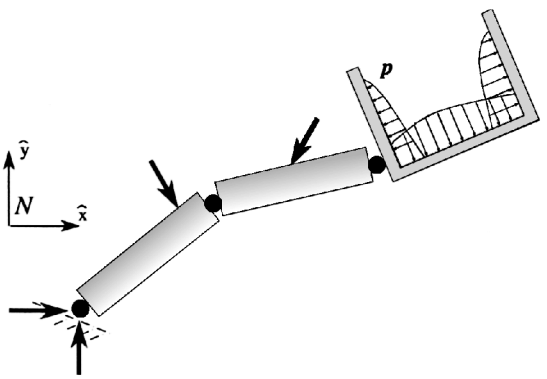

Fig. 2 Structure free-body diagram.

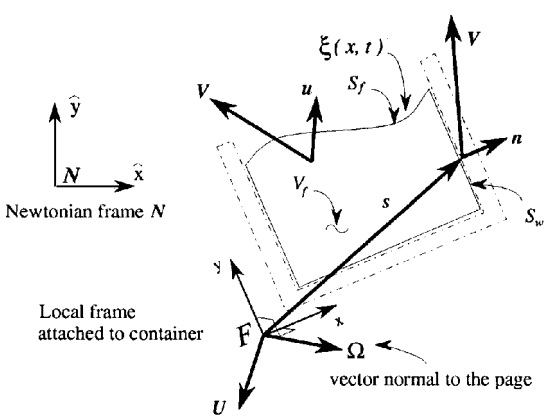

Fig. 3 Nomenclature for a two-dimensional fluid domain.

The pressure on S_f is set to zero without affecting the dynamics. Surface tension effects are not considered in this work. On the wet surface S_w, a kinematic condition for the local velocity $\boldsymbol{u}$ (as seen in the moving frame F) holds:

$$\boldsymbol{u} \cdot \boldsymbol{n} = 0 \quad \text{on} \quad S_w \tag{6}$$

where $\boldsymbol{n}$ is the normal to the surface and $\boldsymbol{u}$ is found from $\boldsymbol{V} = \boldsymbol{U} + \boldsymbol{u} + \boldsymbol{\Omega} \times \boldsymbol{s}$. Vectors $\boldsymbol{U}$ and $\boldsymbol{\Omega}$ are the velocity and angular velocity of the frame F attached to the container; $\boldsymbol{s}$ is the local position vector (Fig. 3). Differentiating Eq. (6) and combining it with the Navier–Stokes equation yields

$$\frac{\partial p}{\partial n} = \rho[\boldsymbol{f} - \dot{\boldsymbol{U}} - 2\boldsymbol{\Omega} \times \boldsymbol{u} - \boldsymbol{\alpha} \times \boldsymbol{s} - \Omega \times (\Omega \times \boldsymbol{s})] \cdot \boldsymbol{n} \quad \text{on} \quad S_w \tag{7}$$

where the container walls are assumed flat. All terms on the right-hand side are known except the acceleration $\dot{\boldsymbol{U}}$ and angular acceleration $\boldsymbol{\alpha}$ of the frame F attached to the container. For curved container walls, there is an additional term involving the radius of curvature of the wall that is not considered here. Intermediate details can be found in Ref. 39. Notice that both $\dot{\boldsymbol{U}}$ and $\boldsymbol{\alpha}$ are functions of the $\dot{\boldsymbol{U}}_s$ of the structure; therefore, the boundary condition on S_w transforms to

$$\frac{\partial p}{\partial n} = b + [E]_{1\times n}\{\dot{U}_s\}_{n\times 1} \tag{8}$$

where b and the row matrix $[E]$ are functions of the Q_s, the U_s, the fluid properties, and the kinematics of the moving frame. As before, n is the number of generalized coordinates describing the structure. All of these parameters are known at the beginning of any time step. At this point, a crucial fact should be noted: p is a linear field of the $\dot{\boldsymbol{U}}_s$; therefore, the pressure can be found as a function of the $\dot{\boldsymbol{U}}_s$.

4. Solution of Pressure Equations

Choosing, for example, the FEM to solve for the pressure field [Eqs. (4), (5), and (8)], the problem transforms into the algebraic system of equations

$$[K]_{m\times m}\{P\}_{m\times 1} = \{G\}_{m\times 1} + [B]_{m\times n}\{\dot{U}_s\}_{n\times 1} \tag{9}$$

where column matrix $\{P\}$ stores m nodal values of the pressure in the fluid domain. Matrices $[K]$, $\{G\}$, and $[B]$ appear naturally in the discretization process. Solving for $\{P\}$ yields

$$\{P\}_{m\times 1} = \{P_0\}_{m\times 1} + [P_1]_{m\times n}\{\dot{U}_s\}_{n\times 1} \tag{10}$$

where $[K]$ has to be assembled at each time step but computations are carried out using a standard solver with $n + 1$ load cases.

5. Coupling the Equations of Structure and Fluid

Building the equations of motion for both structure and fluid involves coupling Eq. (10) with the equations of motion for the structure [Eq. (1)].

In Eq. (1), $\{R\}$ can be split into one column involving the forcing terms not caused by the pressure p and another term including the force and moment produced by the pressure. Equation (1) can be rewritten as

$$[M]_{n\times n}\{\dot{U}_s\}_{n\times 1} = \{J\}_{n\times 1} + [D]_{n\times 3}\{F_x F_y M_z\}^T_{1\times 3} \tag{11}$$

where F_x, F_y, and M_z are the components of the force and moment acting on the rigid container due to the pressure. In the context of Kane, matrix $[D]$ involves components of partial velocities.[35–37] The force and moment due to the pressure are found from

$$(F_x, F_y) = \int_{S_w} p\boldsymbol{n}\, \mathrm{d}S \tag{12}$$

$$M_z = \boldsymbol{k} \cdot \int_{S_w} \boldsymbol{s} \times p\boldsymbol{n}\, \mathrm{d}S \tag{13}$$

Equations (12) and (13) may be evaluated with the same interpolation functions used in solving the boundary-value problem for the pressure [Eq. (9)]. Combining the last two equations with Eq. (10) results in

$$\{F_x F_y M_z\}^T_{1\times 3} = \{I\}_{3\times 1} + [H]_{3\times n}\{\dot{U}_s\}_{n\times 1} \tag{14}$$

and combining this last equation with Eq. (11) leads to

$$[M']_{n\times n}\{\dot{U}_s\}_{n\times 1} = \{J'\}_{n\times 1} \tag{15}$$

where

$$[M']_{n\times n} = [M]_{n\times n} - [D]_{n\times 3}[H]_{3\times n} \tag{16}$$

$$\{J'\}_{n\times 1} = \{J\}_{n\times 1} + [D]_{n\times 3}\{I\}_{3\times 1} \tag{17}$$

Equations (2) and (15) are the desired equations for the coupled system and can be used with an assortment of integration schemes. Solving Eqs. (2) and (15) permits updating the configuration of the structure. Expressions for updating the configuration of the fluid—velocity field and position of the free surface—need to be built.

6. Updating the Free Surface and Velocities

Solving for the $\dot{U}_s$ [Eq. (15)] also permits finding the pressure field using Eq. (10). With the calculated pressure, the accelerations of

the fluid particles can be found by reusing Navier–Stokes equations (other alternatives are possible). One expression for updating the velocity field is

$$\frac{\mathrm{D}\boldsymbol{V}}{\mathrm{D}t} = (-\nabla p + \rho \boldsymbol{f} + \rho\nu\nabla^2\boldsymbol{V})/\rho - (\boldsymbol{V} - \boldsymbol{c})\nabla\boldsymbol{V} \tag{18}$$

Vector $\boldsymbol{c}$ depends on the choice made by the analyst on where to find the updated velocity.

The free surface can be updated using either a Lagrangian or an Eulerian approach. For the latter, the following kinematical condition holds:

$$\frac{\partial \xi}{\partial t} = v - u\frac{\partial \xi}{\partial x} \tag{19}$$

where x is a local coordinate, u and v are the components of the local velocity $\boldsymbol{u}$, and $\xi(x, t)$ describes the free surface position as seen in the moving frame F.

7. Recapitulation

Letting $\boldsymbol{Y} = (U_s, Q_s, \boldsymbol{V}, \xi)^T$ be the configuration of the structure and the fluid, the set of first-order equations of motion for the coupled system is

$$\dot{\boldsymbol{Y}} = \boldsymbol{F}(\boldsymbol{Y}) \tag{20}$$

where $\dot{\boldsymbol{Y}}$ and $\boldsymbol{F}(\boldsymbol{Y})$ are

$$\dot{\boldsymbol{Y}} = \begin{pmatrix} \dot{U}_s \\ \dot{Q}_s \\ \dfrac{\mathrm{D}\boldsymbol{V}}{\mathrm{D}t} \\ \dfrac{\partial \xi}{\partial t} \end{pmatrix} \tag{21}$$

$$\boldsymbol{F}(\boldsymbol{Y}) = \begin{pmatrix} [M']^{-1}\{J'\} \\ [C]\{U_s\} \\ (-\nabla p + \rho \boldsymbol{f} + \rho\nu\nabla^2\boldsymbol{V})/\rho - (\boldsymbol{V} - \boldsymbol{c})\nabla\boldsymbol{V} \\ v - u\dfrac{\partial \xi}{\partial x} \end{pmatrix}$$

The first (top) row of column vector $\boldsymbol{F}(\boldsymbol{Y})$ is evaluated by solving for p [Eqs. (4), (5), and (8)]. Once the accelerations are found, p can be retrieved using Eq. (10) and the third row can be evaluated. The second and fourth rows are kinematic expressions; they are independent of the accelerations. Setting initial conditions for $\boldsymbol{Y}$ poses no difficulties.

8. Commentaries

Details on the numerical implementation of this approach and the implementation of the stream function are the subject of a current work in progress. However, a numerical singularity (boundary value for the pressure) at the intersection of the free surface with the walls of the container leads to instabilities in updating the free-surface position. It can be argued that Poisson's equation for the pressure is not well posed according to the discussion by Gresho and Sani.[40]

B. Potential Flow

1. Motion of the Structure and Velocity Potential

When modeling the fluid as potential flow, the first step is to find the equations of motion for the structure exactly as for the Navier–Stokes model [Eqs. (1) and (2)]. In addition, an intermediate step is needed before building the equation for the pressure, namely, to solve for the velocity potential ϕ. The well-known boundary-value problem is

$$\nabla^2\phi = 0 \quad \text{in} \quad V_f \tag{22}$$

$$\phi = \text{prescribed} \quad \text{on} \quad S_f \tag{23}$$

$$\frac{\partial \phi}{\partial n} = (\boldsymbol{U} + \Omega \times \boldsymbol{s}) \cdot \boldsymbol{n} \quad \text{on} \quad S_w \tag{24}$$

where ϕ and the absolute velocity $\boldsymbol{V}$ of fluid particles are related by $\boldsymbol{V} = \nabla\phi$.

2. Solution of Potential Equations

Using BEM to solve for ϕ, the discrete equations can be written as

$$[K']_{m\times m}\{\Phi\}_{m\times 1} = \{A\}_{m\times 1} \tag{25}$$

Array $\{\Phi\}$ stores both nodal values of the potential on the wet surface and nodal values of the normal derivative of the potential on the free surface. Although the solution for the velocity potential is independent of the $\dot{U}_s$, it must be performed beforehand because the field and boundary equations for the pressure (as will be shown) need the current values of the velocities. Velocities are found by numerically differentiating the values of ϕ.

3. Field Equation for the Pressure

Euler's equation of motion with Rayleigh damping[16,27] is

$$\rho\left[\frac{\partial \boldsymbol{V}}{\partial t} + \frac{1}{2}\nabla(V^2)\right] = -\nabla p + \rho \boldsymbol{f} - \rho\mu\boldsymbol{u} \quad \text{in} \quad V_f \tag{26}$$

where V is the modulus of $\boldsymbol{V}$ and μ is a Rayleigh damping coefficient. Notice the use of $\boldsymbol{u}$ instead of $\boldsymbol{V}$ for the damping term (modified Rayleigh damping). Combining Eq. (26) with the incompressibility condition yields

$$\nabla^2 p = -\tfrac{1}{2}\rho\nabla^2(V^2) \quad \text{in} \quad V_f \tag{27}$$

This is Poisson's equation for the pressure, which can be transformed into Laplace's equation for a variable h defined as $h = p/\rho + (V^2/2)$. Another alternative is to solve Eq. (27) using the BEM by taking care of transforming all domain integrals into surface integrals during the evaluation of the load vector.

4. Boundary Conditions for the Pressure

Following the same derivations as for the Navier–Stokes model and considering an inviscid fluid results in

$$p = 0 \quad \text{on} \quad S_f \tag{28}$$

and on S_w for flat container walls,

$$\frac{\partial p}{\partial n} = \rho[\boldsymbol{f} - \dot{\boldsymbol{U}} - 2\boldsymbol{\Omega}\times\boldsymbol{u} - \boldsymbol{\alpha}\times\boldsymbol{s} - \boldsymbol{\Omega}\times(\boldsymbol{\Omega}\times\boldsymbol{s})]\cdot\boldsymbol{n} \quad \text{on} \quad S_w \tag{29}$$

which analogously transforms into

$$\frac{\partial p}{\partial n} = b' + [E']_{1\times n}\{\dot{U}_s\}_{n\times 1} \tag{30}$$

As before, p is a linear field of the $\dot{U}_s$.

5. Solution of Pressure Equations

Although finding p involves solving a second boundary-value problem, considerable savings in computer time are possible after noticing that the problems for ϕ and p have a similar operator in the field equation and similar types of boundary conditions over the same domain. Therefore, the matrix of coefficients in the BEM equations are the same, and it is practicable to form only the load vector for the solution for p. The already-factorized matrix of coefficients $[K']$ used to solve for the potential ϕ [Eq. (25)] is reused. The BEM equations for p are

$$[K']_{m\times m}\{P\}_{m\times 1} = \{G'\}_{m\times 1} + [B']_{m\times n}\{\dot{U}_s\}_{n\times 1} \tag{31}$$

where $\{P\}$ is a column matrix storing the nodal values of p on S_w and the nodal values of the normal derivative of p on S_f. Solving for $\{P\}$ yields

$$\{P\}_{m\times 1} = \{P_0\}_{m\times 1} + [P_1]_{m\times n}\{\dot{U}_s\}_{n\times 1} \tag{32}$$

where $[K']$ is being reused from the solution for ϕ and the computations to solve for $\{P_0\}$ and $[P_1]$ are carried out as explained in Sec. II.A.4.

6. Coupling the Equations of Structure and Fluid

The coupling of the boundary solution for p and the equations of motion for the structure is the same as for the model using Navier–Stokes equations. An equation similar to Eq. (15) is retrieved, and the solution for the $\dot{U}_s$ allows for updating the configuration of the structure.

7. Updating the Free Surface and Velocity Potential

Updating the value of the potential on the free surface is independent of the solution for the $\dot{U}_s$. For the general motion of the container and Eulerian updating of the free surface, we have

$$\frac{\mathrm{D}\phi}{\mathrm{D}t} = \frac{1}{2}\left[\left(\frac{\partial\phi}{\partial x}\right)^2 + \left(\frac{\partial\phi}{\partial y}\right)^2\right] - u\left(\frac{\partial\phi}{\partial x} + \frac{\partial\phi}{\partial y}\frac{\partial\xi}{\partial x}\right) + f_x\hat{x} + f_y\hat{y} - \mu L \tag{33}$$

where u is the x component of the local velocity $\boldsymbol{u}$ found from $\nabla\phi = \boldsymbol{U} + \boldsymbol{u} + \Omega \times \boldsymbol{s}$. Parameters f_x and f_y are global components of the body force per unit mass $\boldsymbol{f}$, $\hat{x}$ and $\hat{y}$ are global coordinates of the free surface, and L is a potential such that $\nabla L = \boldsymbol{u}$.

When updating the free-surface position using an Eulerian approach, the following kinematic condition holds:

$$\frac{\partial\xi}{\partial t} = v - u\frac{\partial\xi}{\partial x} \tag{34}$$

8. Recapitulation

Letting $\boldsymbol{Y} = (U_s, Q_s, \phi, \xi)^T$ be the configuration, the set of equations of motion is

$$\dot{\boldsymbol{Y}} = \boldsymbol{F}(\boldsymbol{Y}) \tag{35}$$

where $\dot{\boldsymbol{Y}}$ and $\boldsymbol{F}(\boldsymbol{Y})$ are

$$\dot{\boldsymbol{Y}} = \begin{pmatrix} \dot{U}_s \\ \dot{Q}_s \\ \dfrac{\mathrm{D}\phi}{\mathrm{D}t} \\ \dfrac{\partial\xi}{\partial t} \end{pmatrix} \tag{36}$$

$$\boldsymbol{F}(\boldsymbol{Y}) = \begin{pmatrix} [M']^{-1}\{J'\} \\ [C]\{U_s\} \\ \dfrac{1}{2}\left[\left(\dfrac{\partial\phi}{\partial x}\right)^2 + \left(\dfrac{\partial\phi}{\partial y}\right)^2\right] - u\left(\dfrac{\partial\phi}{\partial x} + \dfrac{\partial\phi}{\partial y}\dfrac{\partial\xi}{\partial x}\right) + f_x\hat{x} + f_y\hat{y} - \mu L \\ v - u\dfrac{\partial\xi}{\partial t} \end{pmatrix}$$

The first row of $\boldsymbol{F}(\boldsymbol{Y})$ is evaluated by first solving for ϕ and then solving for p. The third row needs the values of ϕ only. The second and fourth rows are kinematic expressions. Also, the potential L has to be found such that $\nabla L = \boldsymbol{u}$. Initial conditions for $\boldsymbol{Y}$ may require solving for ϕ if the initial $\boldsymbol{V}$ is not zero.

9. Commentaries

The numerical solution for the velocity potential faces two acquainted problems—the singularity existing in the corner where the free surface meets the walls[41] and the instability of the free-surface position.[42] To deal with the first problem, the recommendations in Grilli and Svendsen[17] were followed; and for the second, a smoothing kernel[42] was used. Furthermore, values of the kernel for nodes close to the walls were derived in this work to avoid symmetry assumptions. Taking Fig. 4 as reference, the smoothing kernels are as follows:

1) away from the wall,[42]

$$\bar{f}_i = \frac{-f_{i-2} + 4f_{i-1} + 10f_i + 4f_{i+1} - f_{i+2}}{16}$$

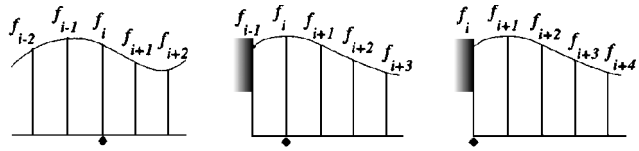

a) Away from the wall b) Near the wall c) At the wall

Fig. 4 Position and nomenclature for smoothing kernels: ♦, Kernel position.

2) near the wall,

$$\bar{f}_i = \frac{3f_{i-1} + 8f_i + 6f_{i+1} - f_{i+3}}{16}$$

3) at the wall,

$$\bar{f}_i = \frac{11f_i + 12f_{i+1} - 6f_{i+2} - 4f_{i+3} + 3f_{i+4}}{16}$$

Potential L introduced in Eq. (33) is a consequence of the introduction of the damping term $\rho\mu\boldsymbol{u}$ instead of $\rho\mu\boldsymbol{V}$ in Eq. (26). L may be replaced by ϕ if the motion of the container is small. For the case of no angular velocity of the container, L is given exactly as

$$L = \phi - U_x x - U_y y \tag{37}$$

where U_x and U_y are the components of the absolute frame velocity in local components. If it is decided to take into account the angular velocity of the frame, L is to be found from

$$\nabla^2 L = 0 \quad \text{in} \quad V_f \tag{38}$$

$$\frac{\partial L}{\partial n} = (\nabla\phi - \boldsymbol{U} - \boldsymbol{\Omega} \times \boldsymbol{s}) \cdot \boldsymbol{n} \quad \text{on} \quad S_f \cup S_w \tag{39}$$

and arbitrarily fixing the value of L at one point. Notice that the right-hand side of Eq. (39) is identically zero on the wet surface. The use of L instead of ϕ guarantees no spurious forces in the solution. See a discussion in Ref. 39.

In deriving the field equation for the pressure [Eq. (27)], it has been assumed that the density and body forces are constant. For variable body forces, it would be necessary to find a potential Ψ such that $\boldsymbol{f} = \nabla\Psi$ and to rebuild Eq. (33) accordingly. An interesting fact about solving Eq. (27) (or its equivalent Laplace's form) is the need to evaluate normal derivatives of $V^2/2$; this proved to be cumbersome and greatly influenced the accuracy of the overall solution.

Another feasible approach to building the coupled equations of motion is to replace the pressure problem by a boundary-value problem for ϕ_t (Ref. 17), obtaining ϕ_t as a function of the accelerations of the container. The pressure could be retrieved using Bernoulli's equation.[13] Other approximate alternatives deal with a gross approximation for ϕ_t or are based on trial-and-error iterations to obtain the interaction pressure.

III. Numerical Examples

The examples presented next were prepared by implementing the methodology using the potential flow model. The BEM was used with three integration schemes, two explicit and one implicit fifth-order Runge–Kutta suitable for stiff systems. Both quadratic and linear elements were employed.

Besides the smoothing routines, two correction procedures were performed, one for maintaining constant volume and the other for compatibility of ϕ:

$$\int_{S_f} \xi \, \mathrm{d}x = \text{const}, \qquad \int_{S_f \cup S_w} \frac{\partial\phi}{\partial n} \, \mathrm{d}S = 0 \tag{40}$$

The code was written to handle rectangular containers. A flag in the data allows for skipping the true interaction and treats the problem as one with prescribed motion of the container; this was done

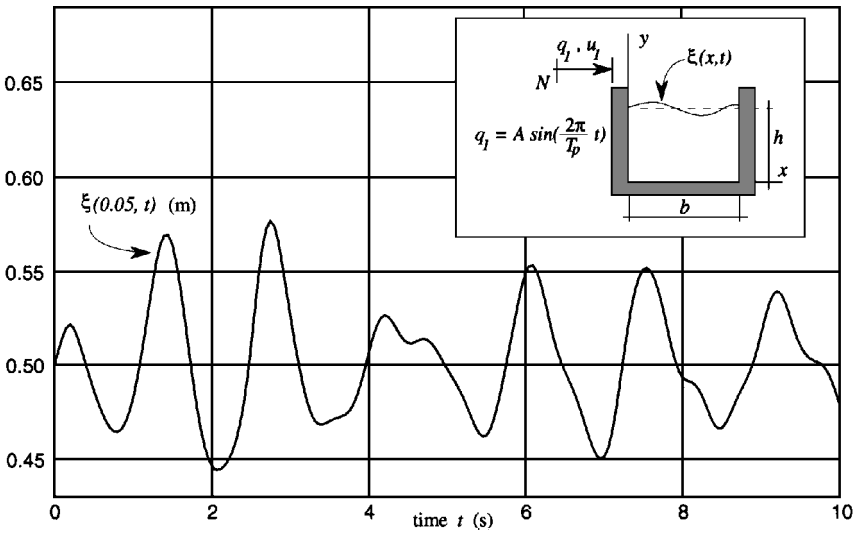

Fig. 5 Prescribed container motion: validation of flow solution.

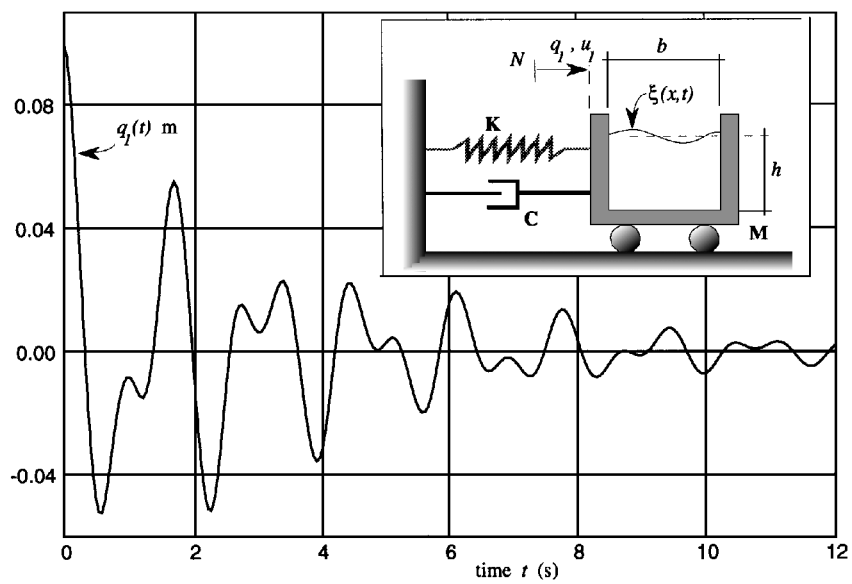

Fig. 6 Container–spring–damper–fluid true interaction.

to validate the flow calculations by comparing the results with other works found in the literature. Satisfactory agreement was found with Faltinsen,[16] Romero and Ingber,[27] and Nakayama and Washizu.[11] One validation problem is shown in Fig. 5, which depicts the results for a prescribed horizontal harmonic motion of the container given by

$$q_1 = A \sin[(2\pi/T_p)t] \tag{41}$$

where $A = 0.025$ m and $T_p = 1.6$ s. Also, $\rho = 1000$ kg/m^3, $b = 1.0$ m (width of container), $h = 0.5$ m (undisturbed liquid height), $\boldsymbol{f} = (0, -9.8)$ m/s^2, and $\mu = 0.05\,\mu_{\text{crit}}$ (Ref. 16). Initial conditions were $\xi(x, 0) = 0.5$ and zero local velocities. Figure 5 shows the plot of the surface elevation at 0.05 m from the left wall relative to time.

A. Container–Spring–Damper–Fluid True Interaction

The simplest true interaction problem is a rigid container coupled with a spring and a damper in rectilinear horizontal motion (see Fig. 6). For this case there is only one ($n = 1$) generalized coordinate q_1, yet it is a clarifying example. The equations of motion for the structure [Eqs. (1) and (2)] are

$$M\dot{u}_1 = -Cu_1 - Kq_1 + F_p \tag{42}$$

$$\dot{q}_1 = u_1 \tag{43}$$

where M is the mass of the container (without the fluid), C is a viscous damping coefficient, K is the spring's stiffness, and F_p is the interaction force due to the pressure. Solving the boundary values for ϕ and p [Eqs. (22) and (27)] leads to

$$\{P\}_{m\times 1} = \{P_0\}_{m\times 1} + \{P_1\}_{m\times 1}\dot{u}_1 \tag{44}$$

[Eq. (32)] and using $\{P_0\}$ and $\{P_1\}$ in Eq. (12) (only the x component is needed in this problem), it is found that the interaction force is

$$F_p = F_0 + F_1\dot{u}_1 \tag{45}$$

The coupled equation of motion (15) is

$$(M - F_1)\dot{u}_1 = -Cu_1 - Kq_1 + F_0 \tag{46}$$

The data for the container were $M = 356$ kg, $K = 20{,}000$ N/m, $C = 266.83$ N·s/m [5% of critical damping $2\sqrt{(KM)}$], width $b = 1.0$ m, and width perpendicular to the paper $E = 1.0$ m. The data for the fluid were $\rho = 1000$ kg/m^3, $\boldsymbol{f} = (0, -9.8)$ m/s^2, and $\mu = 0.05\,\mu_{\text{crit}}$. The initial conditions were $q_1 = 0.10$ m, $u_1 = 0$ m/s, $\xi(x, 0) = 0.5$ m ($h = 0.50$ m), and zero initial fluid local velocities. Figure 6 shows the plot for q_1 vs time. A remarkably similar plot can be found by using the approximate method of Housner[43] in which the container and fluid are modeled as a two-degree-of-freedom system.

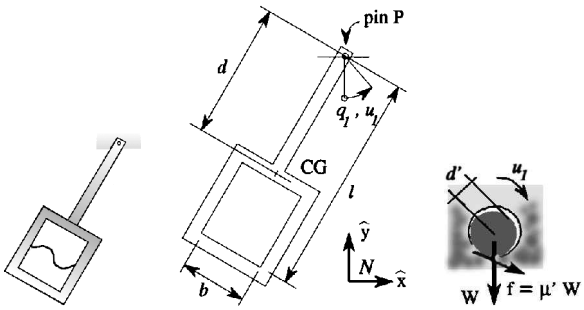

a) Pendulum b) Nomenclature c) Pin *P* details

Fig. 7 Pendulum problem.

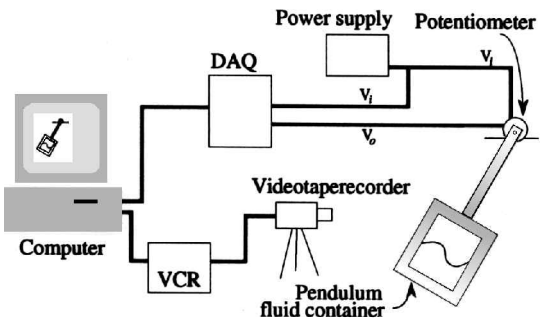

Fig. 8 Experimental setup.

B. Experimental Verification

1. Problem Statement

A rigid-pendulum container was selected for the experimental verification of the methodology (Figs. 7a and 7b). The equations of motion are

$$I\dot{u}_1 = -Cu_1 - gMd\sin(q_1) - M_{\mu'} - M_p \tag{47}$$

$$\dot{q}_1 = u_1 \tag{48}$$

where I and M are the inertia and mass of the pendulum, respectively (without including the fluid), C is a viscous-type damping coefficient, g is the acceleration of gravity, and d is the position of the center of mass. $M_{\mu'}$ is a Coulomb friction moment due to the friction force on the support pin, and M_p is the moment due to the fluid pressure. $M_{\mu'}$ is modeled as

$$M_{\mu'} = fd'(u_1/|u_1|), \qquad f = \mu' W \tag{49}$$

where μ' is a Coulomb friction coefficient (Fig. 7c), d' is the radius of the support pin, and W is either the weight Mg (if the pendulum has no fluid) or $(M + M_l)g$ (if the pendulum has fluid). M_l is the total mass of fluid.

2. Parameter Identification

Directly measured data for the real pendulum were $I = 0.4$ kg·m^2, $M = 1.95$ kg, $d = 0.4$ m, $d' = 0.0125$ m, $b = 0.098$ m, $E = 0.098$ m (container's width normal to page), $g = 9.8$ m/s^2, and $l = 0.543$ m. This left only C and μ' for identification. The identification was performed by running the pendulum with no fluid

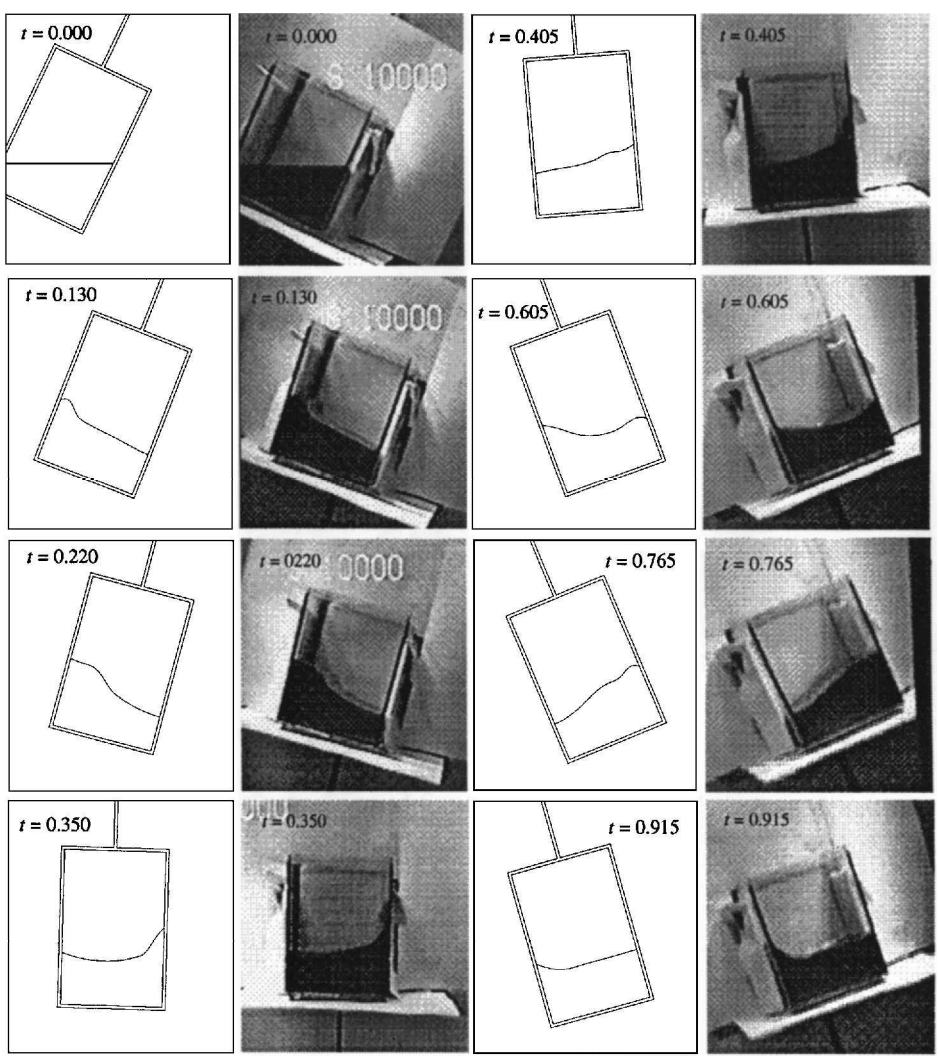

Fig. 9 Numerical results: $t = 0.000$–0.915.

and measuring the angular position q_1 vs time (see setup in Fig. 8). Correspondingly, Eqs. (47) and (48) were solved (setting $M_p = 0$) for different values of C and μ' until matching curves between the numerical and the measured angular positions were obtained. It was found that $C = 0.01$ N · m · s and $\mu' = 0.40$.

The known fluid parameters were $\rho = 1000$ kg/m^3 (water with ink drops) and $\boldsymbol{f} = (0, -9.8)$ m/s^2, and the Rayleigh damping coefficient was estimated to be $0.15\,\mu_{\text{crit}}$. The height of undisturbed fluid was set to $h = 0.049$ m.

3. Numerical Simulation and Experimental Verification

A numerical simulation of the problem was performed with the initial conditions $q_1 = -26$ deg, $u_1 = 0$, and zero initial fluid local velocities. Figure 9 shows a comparison between graphs of the numerical results prepared by an animation code along with snapshots taken from the experiment during the first second of the motion. Besides the highly nonlinear behavior, good agreement can be observed. Beyond 1 s, measured and calculated motion for the fluid and pendulum are also in good agreement. An interesting fact is that at approximately 4.0 s, the fluid is completely damped and the coupled system behaves as a rigid body.

IV. Conclusions

No new contributions have been addressed for modeling the dynamics of the fluid or that of the structure, but a new closed-form methodology for modeling fluid–structure interaction problems is presented. The solution is expedited by building a boundary-value problem for the pressure. The crucial feature of this approach is the linearity of the pressure with respect to the accelerations of the moving frame attached to the fluid domain. The main characteristics of this approach are the following.

1) In the context of this work, a structure means either a single rigid container or a rigid container coupled to a flexible multibody system. The analyst may model a broad class of problems—road containers, robots, aircraft, offshore structures, ship motion.

2) Inherent geometric nonlinearities due to the motion of moving frames attached to bodies are automatically taken into account. Material and geometric nonlinear effects (large displacements) can be implemented.

3) Two fluid models are studied. All nonlinearities in the fluid domain are taken into account. Other fluid models can be implemented. FEM, BEM, and finite differences can be used for solving for the pressure equations.

4) A modified Rayleigh damping approach is introduced.

5) The end result of the methodology is a set of first-order differential equations for the motion of both the fluid and the structure. Diverse integration methods and control laws can be implemented.

Acknowledgments

The authors express gratitude to Sandia National Laboratories for their generous support of this work under Contract AP-7942.

References

[1]Chen, K.-H., and Pletcher, R. H., "Simulation of Three-Dimensional Liquid Sloshing Flows Using a Strongly Implicit Calculation Procedure," *AIAA Journal*, Vol. 31, No. 5, 1993, pp. 901–910.

[2]Hino, T., "Computation of a Free Surface Flow Around an Advancing Ship by the Navier–Stokes Equations," *Proceedings of the 5th International Conference on Numerical Ship Hydrodynamics* (Hiroshima, Japan), edited by K. Mori, National Academy Press, Washington, DC, 1990, pp. 103–117.

[3]Hoekstra, M., "Recent Developments in a Ship Stern Flow Prediction Code," *Proceedings of the 5th International Conference on Numerical Ship Hydrodynamics* (Hiroshima, Japan), edited by K. Mori, National Academy Press, Washington, DC, 1990, pp. 87–101.

[4]Miyata, H., Sato, T., and Baba, N., "Difference Solution of a Viscous Flow with Free-Surface Wave About an Advancing Ship," *Journal of Computational Physics*, Vol. 72, 1987, pp. 393–421.

[5]Popov, G., Sankar, S., Sankar, T. S., and Vatistas, G. H., "Liquid Sloshing in Rectangular Road Containers," *Computers and Fluids Journal*, Vol. 21, No. 4, 1992, pp. 551–569.

[6]Zhu, M., Miyata, H., and Kajitani, H., "Finite-Difference Simulation of a Viscous Flow About a Ship of Arbitrary Configuration," *Proceedings of the 5th International Conference on Numerical Ship Hydrodynamics* (Hiroshima, Japan), edited by K. Mori, National Academy Press, Washington, DC, 1990, pp. 119–131.

[7]Agrawal, B. N., "Dynamic Characteristics of Liquid Motion in Partially Filled Tanks of a Spinning Spacecraft," *Journal of Guidance, Control, and Dynamics*, Vol. 16, No. 4, 1993, pp. 636–640.

[8]Casciola, C. M., and Piva, R., "A Boundary Integral Formulation for Free Surface Viscous and Inviscid Flows About Submerged Bodies," *Proceedings of the 5th International Conference on Numerical Ship Hydrodynamics* (Hiroshima, Japan), edited by K. Mori, National Academy Press, Washington, DC, 1990, pp. 469–479.

[9]Casciola, C. M., and Piva, R., "A Boundary Integral Approach in Primitive Variables for Free Surface Flows," *Proceedings of the 18th Symposium on Naval Hydrodynamics*, National Academy Press, Washington, DC, 1991, pp. 221–237.

[10]Bai, K. J., Kim, J. W., and Kim, Y. H., "Numerical Computations for a Nonlinear Free Surface Flow Problem," *Proceedings of the 5th International Conference on Numerical Ship Hydrodynamics* (Hiroshima, Japan), edited by K. Mori, National Academy Press, Washington, DC, 1990, pp. 403–419.

[11]Nakayama, T., and Washizu, K., "Nonlinear Analysis of Liquid Motion in a Container Subjected to Forced Pitching Oscillation," *International Journal for Numerical Methods in Engineering*, Vol. 15, 1980, pp. 1207–1220.

[12]Ru-De, F., "Finite Element Analysis of Lateral Sloshing Response in Axisymmetric Tanks with Triangular Elements," *ComputationalMechanics*, Vol. 12, 1993, pp. 51–58.

[13]Cointe, R., Geyer, P., King, B., Molin, B., and Tramoni, M., "Nonlinear and Linear Motions of a Rectangular Barge in a Perfect Fluid," *Proceedings of the 18th Symposium on Naval Hydrodynamics*, National Academy Press, Washington, DC, 1991, pp. 85–99.

[14]Cointe, R., Molin, B., and Nays, P., "Nonlinear and Second-Order Transient Waves in a Rectangular Tank," *BOSS'88: Proceedings of the International Conference on Behavior of Offshore Structures* (Trondheim, Norway), Tapir, Trondheim, Norway, 1988, pp. 705–718.

[15]Dommermuth, D. G., and Yue, D. K. P., "Numerical Simulations of Nonlinear Axisymmetric Flows with a Free Surface," *Journal of Fluid Mechanics*, Vol. 178, 1987, pp. 195–219.

[16]Faltinsen, O. M., "A Numerical Nonlinear Method of Sloshing in Tanks with Two-Dimensional Flow," *Journal of Ship Research*, Vol. 22, No. 3, 1978, pp. 193–202.

[17]Grilli, S. T., and Svendsen, I. A., "Corner Problems and Global Accuracy in the Boundary Element Solution of Nonlinear Wave Flows," *Engineering Analysis with Boundary Elements*, Vol. 7, No. 4, 1990, pp. 178–195.

[18]Hwang, J. H., Kim, I. S., Seol, Y. S., Lee, S. C., and Chon, Y. K., "Numerical Simulation of Liquid Sloshing in Three-Dimensional Tanks," *Computers and Structures*, Vol. 44, No. 1/2, 1992, pp. 339–342.

[19]Hwang, J. H., Kim, Y. J., and Kim, S. Y., "Nonlinear Hydrodynamic Forces Due to Two-Dimensional Forced Oscillation," *Nonlinear Water Waves IUTAM Symposium* (Tokyo, Japan), Springer–Verlag, Berlin, 1988, pp. 231–238.

[20]Lin, W.-M., Newman, J. N., and Yue, D. K., "Nonlinear Forced Motions of Floating Bodies," *Fifteenth Symposium Naval Hydrodynamics: Seakeeping Problems, Hull Propeller Interactions, Nonlinear Free-Surface Problems, Frontier Problems in Hydrodynamics*, National Academy Press, Washington, DC, 1985, pp. 33–49.

[21]Liu, P. L., and Liggett, J. A., "Applications of Boundary Element Methods to Problems of Water Waves," *Developments in Boundary Element Methods*, edited by P. K. Banerjee and R. P. Shaw, Vol. 2, Applied Science, London, 1982, pp. 37–67.

[22]Liu, P. L., and Liggett, J. A., "Boundary Element Formulations and Solutions for Some Non-Linear Water Wave Problems," *Developments in Boundary Element Methods*, edited by P. K. Banerjee and S. Murkerjee, Vol. 3. Applied Science, London, 1984, pp. 171–190.

[23]Nakayama, T., "Boundary Element Analysis of Nonlinear Water Wave Problems," *International Journal for Numerical Methods in Engineering*, Vol. 19, 1983, pp. 953–970.

[24]Nakayama, T., and Tanaka, H., "A Numerical Method for the Analysis of Nonlinear Sloshing in Circular Cylindrical Containers," *Boundary Integral Methods, Theory and Applications: Proceedings of the IABEM Symposium* (Rome, Italy), edited by L. Morino and R. Piva, Springer–Verlag, Berlin, 1991, pp. 359–368.

[25]Nakayama, T., and Washizu, K., "Boundary Element Analysis of Non-Linear Sloshing Problems," *Developments in Boundary Element Methods*, edited by P. K. Banerjee and S. Murkerjee, Vol. 3, Applied Science, London, 1984, pp. 191–211.

[26]Nestegard, A., and Sclavounos, P. D., "A Numerical Solution of Two-Dimensional Deep Water Wave-Body Problems," *Journal of Ship Research*, Vol. 28, No. 1, 1984, pp. 48–54.

[27]Romero, V. J., and Ingber, M. S., "A Numerical Model for 2-D Sloshing of Pseudo-Viscous Liquids in Horizontally Accelerated Rectangular Containers," *Proceedings of the 17th International Conference on Boundary Elements* (Madison, WI), edited by C. Brebbia, Computational Mechanics Publications, Southampton, England, UK, 1995, pp. 567–583.

[28]Lui, A. P., and Lou, J. Y. K., "Dynamic Coupling of a Liquid-Tank System Under Transient Excitations," *Ocean Engineering*, Vo. 17, No. 3, 1990, pp. 263–277.

[29]Falch, S., "Slamming of Flat-Bottomed Bodies Calculated with Exact Free Surface Boundary Conditions," *Proceedings of the 5th International Conference on Numerical Ship Hydrodynamics* (Hiroshima, Japan), edited by K. Mori, National Academy Press, Washington, DC, 1990, pp. 251–267.

[30]Sen, D., Pawlowski, J. S., Lever, J., and Hinchey, M. J., "Two-Dimensional Numerical Modelling of Large Motions of Floating Bodies in Waves," *Proceedings of the 5th International Conference on Numerical Ship Hydrodynamics* (Hiroshima, Japan), edited by K. Mori, National Academy Press, Washington, DC, 1990, pp. 351–373.

[31]Abramson, H. N., "The Dynamic Behavior of Liquids in Moving Containers with Applications to Space Vehicle Technology," NASA SP-106, 1966.

[32]Morand, H. J. P., and Ohayon, R., *Fluid Structure Interaction: Applied Numerical Methods*, Wiley, New York, 1995.

[33]Crolet, J. M., and Ohayon, R. (eds.), *Computational Methods for Fluid-Structure Interaction*, Pitman Research Notes in Mathematics Series, Wiley, New York, 1994.

[34]Sankar, S., Ranganathan, R., and Rakheja, S., "Impact of Dynamics Fluid Slosh Loads on the Directional Response of Tank Vehicles," *Vehicle System Dynamics*, Vol. 21, 1992, pp. 385–404.

[35]Kane, T. R., and Levinson, D. A., *Dynamics: Theory and Applications*, McGraw–Hill, New York, 1985.

[36]Kane, T. R., Linkins, P. W., and Levinson, D. A., *Spacecraft Dynamics*, McGraw–Hill, New York, 1983.

[37]Barhorst, A. A., and Everett, L. J., "Modeling Hybrid Parameter Multiple Body Systems: A Different Approach," *International Journal of Non-Linear Mechanics*, Vol. 30, No. 1, 1995, pp. 1–21.

[38]Fletcher, C. A. J., *Computational Techniques for Fluid Dynamics*, 2nd ed., Vols. 1 and 2, Springer–Verlag, New York, 1991.

[39]Ortiz, J. L., "Modeling Flexible Multibody Systems–Fluid Interaction," Ph.D. Thesis, Mechanical Engineering Dept., Texas Tech Univ., Lubbock, TX, Dec. 1996.

[40]Gresho, P. M., and Sani, R. L., "On Pressure Boundary Conditions for the Incompressible Navier–Stokes Equations," *International Journal for Numerical Methods in Fluids*, Vol. 7, 1987, pp. 1111–1145.

[41]Lin, W.-M., "Nonlinear Motion of the Free Surface Near a Moving Body," Ph.D. Thesis, Ocean Engineering Dept., Massachusetts Inst. of Technology, Cambridge, MA, Sept. 1984.

[42]Longuett-Higgins, M. S., and Cokelet, E., "The Deformation of Steep Surface Waves on Water I. A Numerical Method of Computation," *Proceedings of the Royal Society of London, Series A: Mathematical and Physical Sciences*, Vol. 350, 1976, pp. 1–26.

[43]Housner, G. W., "The Dynamic Behavior of Water Tanks," *Bulletin of the Seismological Society of America*, Vol. 53, No. 2, 1963, pp. 381–387.